alcohol excited molecules reradiating are known only to an order of magnitude.

### (c) Argon-Ethyl Acetate

Argon-ethyl acetate results at 40 mm Hg and 200 mm Hg total pressures, with 10 percent quenching vapor, show longer plateaus that those for the argon-ethyl alcohol mixtures. For example, at 40 mm Hg, the ethyl alcohol plateau is only about 5 volts wide, whereas the acetate plateau is about 40 volts wide. The value of $C$, determined for ethyl acetate from the preceding equations, was about $1.1\times10^5$, or approximately the same as $C$ for ethyl alcohol, where $C$ was $1\times10^5$. To explain the difference in plateau widths obtained between ethyl alcohol and ethyl acetate, a difference of only 10 percent in the value of $C$ is required. However, this is within the experimental error, and, therefore, further conclusions cannot be made. The value of $D$ was the same for ethyl acetate as for ethyl alcohol, within the experimental error.

### ACKNOWLEDGMENTS

The authors wish to thank Professor F. A. Grant for much valuable information concerning metastable atoms and Professor R. D. Myers for his many helpful discussions during the course of this work.

PHYSICAL REVIEW VOLUME 98, NUMBER 2 APRIL 15, 1955

# High-Frequency Gas Discharge Plasma in Hydrogen*

DAVID J. ROSE, *Bell Telephone Laboratories, Murray Hill, New Jersey*

AND

SANBORN C. BROWN, *Department of Physics and Research Laboratory of Electronics, Massachusetts Institute of Technology, Cambridge, Massachusetts*

(Received January 13, 1955)

The high-frequency electric field required to maintain a hydrogen plasma has been measured as a function of pressure and plasma electron density. A theory of the plasma based on a solution of the Boltzmann transport equation has been developed to predict this field; it agrees satisfactorily with experiment. The theory has no adjustable parameters, and uses only the probabilities of collision, excitation, and ionization of the gas by electrons, and the ionic mobility.

## I. INTRODUCTION

MACDONALD and Brown[1] developed a theory of the mechanism of breakdown in hydrogen at high frequencies that is based on a solution of the Boltzmann transport equation. Calculated breakdown fields agree well with their experimental results. More recently, Allis and Brown[2] (A-B) simplified the method of solution and calculation of the high-pressure case, in which electrons diffusing from the discharge do not remove an appreciable fraction of the total energy. This simplified method may also be applied to the calculation of breakdown in certain other gases. The present paper generalizes these theories by taking into account the effect of space charge, so that it will be possible to compute from first principles the microwave field strength required to maintain certain simple plasmas in the steady state. Calculations made on this basis will be compared with experimental measurements obtained for hydrogen.

The theory presupposes that the following additional nonlinear phenomena peculiar to some plasmas and not to breakdown may be neglected: (a) cumulative ionization, (b) electron-ion recombination, (c) formation of negative ions in appreciable numbers, (d) electron-electron interactions, (e) plasma resonance. These restrictions place an upper limit on the plasma electron density for which the theory is applicable. Limits arising from (a), (b), and (c) may be readily calculated. Regarding limit (d), the work of Haseltine[3] shows that the electron-electron interaction has least effect in gases in which the collision frequency of electrons is independent of electron energy. *A posteriori* calculations show that for hydrogen limit (e) actually controls in our experiments, at frequencies of about 3000 Mc/sec, above a density limit of about $10^{11}/cm^3$, a value well above those experimentally obtained here.

The physical process is the following: Electrons gain energy from the applied field, and lose energy by elastic and inelastic collisions. Ionization of gas molecules provides a source of new electrons, and flow to the tube walls in the presence of density and space-charge potential gradients provides the sink. The Boltzmann transport equation in phase space expresses these balances both in energy and in number; correspond-

* This work was supported in part by the Signal Corps; the Office of Scientific Research, Air Research and Development Command; and the Office of Naval Research.

[1] A. D. MacDonald and S. C. Brown, Phys. Rev. **76**, 1634 (1949).

[2] W. P. Allis and S. C. Brown, Phys. Rev. **87**, 419 (1952).

[3] W. R. Haseltine, J. Math. Phys. **18**, 174 (1939).

ingly, a solution is obtained by splitting it into two parts.

The energy part will contain certain constant spatial parameters describing the space-charge field and diffusion length, and will yield the electron velocity distribution. The spatial part will contain other constant energy parameters (electron diffusion, mobility, and ionization rate), and will give the current and space distributions. The complete solution is obtained by making these various parameters self-consistent.

The problem of the spatial distributions and current flow have been treated by Allis and Rose[4] (A-R) and these results will be used here. The effect of the space-charge field upon the energy distribution, from which the ionization rate is to be computed, must now be considered.

## II. THE BOLTZMANN EQUATION

The development of the Boltzmann equation will follow the work of A-B as closely as possible, and their notation will be used. The only difference is that a dc space-charge field $E_s$ must be superimposed on the high-frequency field so that

$$\mathbf{E}=\mathbf{E}_s+\mathbf{E}_p\exp(j\omega t), \tag{1}$$

where $E_s$ varies with position, but $E_p$ is assumed constant. The distribution $F$ of electrons in velocity and configuration space is then determined by the Boltzmann equation

$$\partial F/\partial t=C-\nabla_r\cdot\mathbf{v}F+\nabla_v\cdot e\mathbf{E}F/m. \tag{2}$$

Here, $C$ represents the effect of collisions; $\nabla_r$ and $\nabla_v$ are the gradient operators in configuration and velocity space; and $v$, $e$, and $m$ are the velocity, charge, and mass of the electron. Following A-B, $F$ is expanded in spherical harmonics in velocity space and a Fourier series in time:

$$\begin{aligned}F&=\textstyle\sum_l\sum_k F_k^l P_l(\cos\theta)\exp(jk\omega t),\\&=F_0^0+\mathbf{v}\cdot[\mathbf{F}_0'+\mathbf{F}_1'\exp(j\omega t)]/v.\end{aligned} \tag{3}$$

It may be shown that the three indicated items suffice for the expansion discussed by Allis and Brown, even if space charge is present, provided that the electron density is sufficiently low that plasma resonance is not encountered.

Allis and Brown have evaluated the collision terms, and have separated the various harmonic terms of the distribution. There are one scalar and two vector equations:

$$\begin{aligned}(\nu_x+\nu_i-q)F_0^0=&-(v/3)\nabla_r\cdot\mathbf{F}_0'+(1/v)^2\partial\{[ev^2/6m]\\&\times[(\mathbf{E}_p\cdot\mathbf{F}_1')_{\text{real}}+2\mathbf{E}_s\cdot\mathbf{F}_0']\\&+[m/M]\nu_c v^3F_0^0\}/\partial v,\end{aligned} \tag{4}$$

$$\nu_c\mathbf{F}_0'=-v\nabla_r F_0^0+(e/m)\mathbf{E}_s\partial F_0^0/\partial v, \tag{5}$$

$$(\nu_c+j\omega)\mathbf{F}_1'=(e\mathbf{E}_p/m)\partial F_0^0/\partial v. \tag{6}$$

[4] W. P. Allis and D. J. Rose, Phys. Rev. **93**, 84 (1954).

Here, $\nu_c$, $\nu_x$, and $\nu_i$ are the collision frequencies of an electron for momentum transfer, excitation, and ionization, respectively. The quantity $qF_0^0$ is the rate of appearance of new electrons at low energies as a result of excitation and ionization; it is permissible to set it equal to a delta function at the origin of velocity space. Except for the additional field $\mathbf{E}_s$, these equations are identical with Eqs. (5), (6), and (7) of A-B.

## III. SEPARATION OF $F$ IN SPACE AND ENERGY

A solution of Eqs. (4)–(6) is possible if $F$ may be separated into spatial and energy parts, $F=N(\mathbf{r})f(v)$. This means, in effect, that the velocity distribution must be the same everywhere in the discharge, and therefore that the diffusion coefficient and mobility are constant.

It is possible to obtain the set of spatial equations by integrating Eqs. (4) and (5) over velocity space. The dc electron particle current,

$$\mathbf{\Gamma}=\int_0^\infty\mathbf{F}_0'(4\pi v^3/3)dv=-\nabla_r(D_-N)-\mu_-\mathbf{E}_sN, \tag{7}$$

is determined by $\mathbf{F}_0'$ from Eq. (5). Here $N$ is the electron spatial density, and the diffusion and mobility coefficients are

$$D_-N=\int_0^\infty(v^2/3\nu_c)F_0^0 4\pi v^2dv; \tag{8}$$

$$\mu_-N=\int_0^\infty(4\pi/3)(e/m)F_0^0[\partial(v^3/\nu_c)/\partial v]dv. \tag{9}$$

The total excitation and ionization rates are

$$N\langle\nu_x\rangle=\int_0^\infty\nu_xF_0^0 4\pi v^2dv, \tag{10}$$

$$N\langle\nu_i\rangle=\int_0^\infty\nu_iF_0^0 4\pi v^2dv; \tag{11}$$

also

$$N(\langle\nu_x\rangle+2\langle\nu_i\rangle)=\int_0^\infty qF_0^0 4\pi v^2dv \tag{12}$$

represents the appearance of all new electrons. Equation (4) may be multiplied by $4\pi v^2dv$ and integrated over all velocities. The term in braces vanishes at both limits, leaving

$$N\langle\nu_i\rangle=\nabla_r\cdot\mathbf{\Gamma}. \tag{13}$$

There is, in addition, an equation for the ion particle current which in the steady state also equals $\mathbf{\Gamma}$:

$$\mathbf{\Gamma}=-\nabla_r(D_+P)+\mu_+\mathbf{E}_sP, \tag{14}$$

where $P$ is the ion density. Finally, Poisson's equation

$$\nabla_r\cdot\mathbf{E}_s=e(P-N)/\epsilon_0 \tag{15}$$

must hold. Equations (7), (13)–(15) determine the spatial distributions from which the average ionization frequency per electron $\langle\nu_i\rangle$ is determined as a characteristic value. It is these equations, with constant $D$'s and $\mu$'s, that have been treated by Allis and Rose.

The presence of certain crossed space and velocity terms in Eqs. (4)–(6) indicate that the separation of $F$ into a product $N(r)F(v)$ is not quite correct. It will now be shown, however, that the dependence of $f(v)$ on space is weak, so that the separation is a good approximation. First, the magnitudes of the terms $(\mathbf{E}_p\cdot\mathbf{F}_1')_{\text{real}}$ and $2\mathbf{E}_s\cdot\mathbf{F}_0'$ are compared. The first represents the energy gain of the electrons from the applied alternating field, and the second their energy loss in flowing against the space-charge field. At values of $p\Lambda>1$ each electron gains energy from $E_p$ sufficient for many exciting collisions and one ionizing collision, in addition to that required to overcome the elastic recoil losses. This total energy is many times the wall potential, so that the space-charge term in Eq. (4) is negligible. The $\mathbf{E}_s$ term in Eq. (5), however, cannot be dismissed, for it represents an inward mobility flow that almost cancels the outward diffusion term.

Equations (5) and (6) are substituted in Eq. (4), giving

$$\begin{aligned}(\nu_x+\nu_i-q)F_0^0=&(v^2/3\nu_c)\nabla_r^2F_0^0\\&-(ev/3m\nu_c)\nabla_r\cdot(\mathbf{E}_s\partial F_0^0/\partial v)\\&+(1/v)^2\partial[(eu_c/3m)\nu_cv^2(\partial F_0^0/\partial v)\\&+m\nu_cv^3F_0^0/M]/\partial v,\end{aligned}\quad(16)$$

where

$$u_c=eE_p^2/2m(\nu_c^2+\omega^2).\quad(17)$$

The terms of Eq. (16) represent, in order, the excitation and ionization processes, diffusion, the counteracting space-charge mobility, energy gain from the applied field, and elastic recoil.

In cases where the electron density is low, $\mathbf{E}_s$ is small, and only the diffusion term contains spatial derivatives. Equation (16) then separates with $\nabla_r^2F_0^0=-F_0^0/\Lambda^2$, where $\Lambda$ is the cavity diffusion length. The spatial distribution is determined by the diffusion equation. On the other hand, when $N$ and $\mathbf{E}_s$ are large, the mobility and diffusion terms nearly cancel, and their difference is small compared to the other terms in the equation; an approximation for the small difference will therefore suffice. A separation is still possible provided only that $\mathbf{E}_sN\sim\nabla_rN$, in which case $\nabla_r^2N=-N/\Lambda^2$ as before. This solution of the space equations is the constant ratio approximation discussed by Allis and Rose. It is correct both at very low and very high electron densities, but is somewhat in error at intermediate densities.

We assume, then, that

$$\mathbf{E}_s=-u_s\nabla N/N,\quad(18)$$

where $u_s$ is a measure of the space charge. We shall also define the electron energy $u=mv^2/2e$ in electron-volts; from Eq. (16), one then obtains

$$\begin{aligned}&(\nu_x+\nu_i-q)f+(2eu/3m\nu_c\Lambda^2)(f+u_sdf/du)\\&\quad=(2/3\sqrt{u})d[u^{\frac{3}{2}}\nu_c(u_cdf/du+3mf/M)]/du.\end{aligned}\quad(19)$$

Let an effective field $E_e$ be defined as

$$E_e^2=\nu_c^2E_p^2/2(\nu_c^2+\omega^2).\quad(20)$$

When the specific dependences of $\nu_x$, $\nu_i$, and $\nu_c$ are inserted, Eq. (19) may be solved to yield a relation between the three parameters $p/E_e$, $E_e\Lambda$, and $u_s$. Furthermore, Eq. (19) may be multiplied by $4\pi v^2dv$ and integrated over all velocities. The right side vanishes, and from Eqs. (8)–(12)

$$D_--u_s\mu_-=\langle\nu_i\rangle\Lambda^2\equiv D_s,\quad(21)$$

which defines $D_s$, the effective diffusion coefficient. The escape frequency of electrons, measured by $D_s/\Lambda^2$, is reduced from the free diffusion frequency $D_-/\Lambda^2$ on account of the space-charge field measured by $u_s$; $\langle\nu_i\rangle$ is correspondingly reduced, and so is the field $E_e$ which maintains the ionization. Thus $p/E_e$ rises in the steady state over the breakdown value.

From the solution of Eqs. (19) and (21), $D_-$, $\mu_-$ and $D_s/D_-$ may be computed as functions of $p/E_e$ and $E_e\Lambda$. Since Allis and Rose give $D_s/D_-$ as a function of $N_0\Lambda^2\mu_-/D_-$, where $N_0$ is the electron density at the center of a parallel plane cavity, it is possible to plot contours of constant $N_0\Lambda^2$ on the $p/E_e-E_e\Lambda$ plane. The special case $N_0\Lambda^2=0$, whence $D_s/D_-=1$ and $u_s=0$, corresponds to breakdown.

## IV. SOLUTION OF THE ENERGY DISTRIBUTION

It is convenient to consider solutions of Eq. (19) for the case of large $p\Lambda$ (greater than 1 mm Hg×cm) and small $p\Lambda$ (between 0.1 and 1.0 mm Hg×cm) separately. All of the experimental measurements were taken within the limit of validity of diffusion theory.[5]

At large values of $p\Lambda$, hence also of $E_e\Lambda$, the escape frequency is low, and the effect of the current flow on the energy distribution becomes small. Correspondingly, the second term of Eq. (19), being in ratio $1/(p\Lambda)^2$ to the remaining terms, is small. In this range, $f$ is determined principally by the balance between energy gain and elastic recoil loss, since there are few electrons in the inelastic range. If $\nu_c$ is independent of electron energy, as is approximately the case with hydrogen, $f$ is close to Maxwellian. The small second term of Eq. (19) can then be approximated by replacing $df/du$ by $-\mu_-f/D_-$, which is true in the average in any case. With the aid of Eq. (21), Eq. (19) becomes

$$\begin{aligned}&(\nu_x+\nu_i-q)f+(2eu/3m\nu_c\Lambda_e^2)f\\&\quad=(2/3\sqrt{u})d[u^{\frac{3}{2}}\nu_c(u_cdf/du+3mf/M)]du,\end{aligned}\quad(22)$$

where

$$\Lambda_e^2=\Lambda^2D_-/D_s\quad(23)$$

[5] S. C. Brown and A. D. MacDonald, Phys. Rev. **76**, 1629 (1949).

defines an effective diffusion length that is larger than the actual cavity diffusion length when the space-charge field is important. Equation (22) is the breakdown equation of A-B for a cavity of diffusion length $\Lambda_e$, and the existing methods of solution may be applied directly. Steady-state values of $E_e\Lambda$ *vs* $p/E_e$ will be replicas of the breakdown values, shifted to lower $E_e\Lambda$ by the ratio $(D_s/D_-)^{\frac{1}{2}}$.

At lower values of $p\Lambda$, hence also of $E_e\Lambda$ and $p/E_e$, the diffusion term is not negligible, and simple approximations cannot be made for it. It is then necessary to develop solutions of the general sort derived in reference 1. This has been done for the case of constant $\nu_c$. Define the parameter

$$\sigma=(2m/M)-(2eu_s/3m\nu_c^2\Lambda^2), \tag{24}$$

which is positive at large $p\Lambda$, and negative at small $p\Lambda$ and large $u_s$. Different solutions are required, depending on the sign of $\sigma$. They differ only in slight mathematical detail; thus, in the following, let $\sigma=|\sigma|$. Then the upper and lower signs, where applied, represent the positive and the negative cases, respectively. The special case $\sigma=0$ has no particular significance.

Define the additional parameters:

$$u_e=2u_c/3\sigma, \tag{25}$$

$$1/\beta^2=1+(2u_e/E_e\Lambda)^2, \tag{26}$$

$$Q=6(2m/\sigma M-1), \tag{27}$$

and a new energy variable

$$z=u/u_e\beta. \tag{28}$$

The quantity $q$ in Eq. (19) will be set equal to a delta function at the origin, and the excitation plus ionization rate will be approximated by

$$\nu_x+\nu_i=\nu_c h_x(u-u_x), \tag{29}$$

where $u_x$ is the first excitation potential. Equation (19) is now expressed in normal form in terms of the variable $z$, so that

$$f=z^{-\frac{1}{2}}g\exp(\mp\beta z/2), \tag{30}$$

$$d^2g/dz^2=[A^2+B/z-3/16z^2]g, \tag{31}$$

where

$$A^2=(\sigma+4h_xu_e\beta^2)/4\sigma, \tag{32}$$

$$B=[(Q\pm3)\sigma\beta+4h_xu_e\beta^2z_x]/4\sigma. \tag{33}$$

The body of the distribution function is that part lying below $u_x$; in that region $\nu_x=\nu_i=0$, and one must set $h_x=0$ in Eqs. (31)–(33). The solution in the body is then

$$f=\exp[-z(1\pm\beta)/2][-CM_1(z)+M_2(z)], \tag{34}$$

where

$$M_1=M\{[3-(Q\pm3)\beta]/4;3/2;z\}, \tag{35}$$

$$M_2=z^{-\frac{1}{2}}M\{[1-(Q\pm3)\beta]/4;1/2;z\}, \tag{36}$$

and $M(\alpha;\gamma;z)$ is the confluent hypergeometric function.[6] The constant $C$ will be determined later.

The tail of the distribution lies above $u_x$, and the function is given by Eqs. (31)–(33) directly. Rather than solving exactly, it is much simpler to use the asymptotic expansion

$$g=\exp(-Az)z^b(1-d/z+\cdots). \tag{37}$$

The invariant $I$ of Eq. (37) is

$$I=A^2-2Ab/z-(1/z)^2[b-b^2+2Ad/(1-d/z)-2bd/z(1-d/z)+2d/z(1-d/z)], \tag{38}$$

which is to be fitted as well as possible to the invariant of Eq. (31). Thus

$$b=B/2A, \tag{39}$$

satisfying the term in $1/z$. The remaining term in $1/z^2$ will be set equal to $\frac{3}{16}$ at $z=z_x$, so that

$$1/d=[2A-2(b-1)/z_x]/[b(b-1)+\tfrac{3}{16}]+1/z_x. \tag{40}$$

Above $u_x$, we have, then,

$$f=R[\exp(-Sz)]z^T(1-d/z), \tag{41}$$

where

$$S=A+(\beta/2), \tag{42}$$

$$T=b-\tfrac{3}{4}. \tag{43}$$

Here, $R$ and $C$ are determined by matching value and slope of $f$ at $z_x$. The derivative $M_2'(z)$ can be eliminated by use of the Wronskian

$$W(z)=M_1'M_2-M_2'M_1=[\exp(z)]/2z^{\frac{1}{2}}. \tag{44}$$

Then

$$R=\frac{\exp[z_x(1-\beta)/2]\exp Sz_x}{2z_x{}^V(1-d/z_x)[M_1'(z_x)+KM_1(z_x)]}, \tag{45}$$

$$C=\{M_2'(z_x)-(\exp z_x)/2z_x[M_1'(z_x)+KM_1(z_x)]\}/M_1(z_x), \tag{46}$$

where

$$V=T+\tfrac{3}{2}, \tag{47}$$

$$K=A-\tfrac{1}{2}-[T+d/z_x(1-d/z_x)]/z_x. \tag{48}$$

The distribution function $f$ is now determined. There are two methods at hand for completing the solution. One method consists, first, of computing $D_-$ and $\mu_-$ from Eqs. (8) and (9), the integration being performed numerically.

One may set, similarly to Eq. (29),

$$\nu_i=\nu_c h_i(u-u_i), \tag{49}$$

where $u_i$ is the ionization potential. Then

$$\langle\nu_i\rangle=\nu_c h_i\int_{u_i}^{\infty}(u-u_i)f4\pi v^2dv$$

$$=2\pi\nu_c h_i R(2e/m)^{\frac{1}{2}}(u_e\beta)^{5/2}\times\int_{z_i}^{\infty}[\exp(-Sz)]z^T(1-d/z)(z-z_i)dz. \tag{50}$$

[6] A. D. MacDonald, J. Math. Phys. **28**, 183 (1949).

Let

$$y=Sz. \tag{51}$$

The integral in Eq. (50) may be performed by parts and expressed in terms of the incomplete gamma function[7] $I(y_i; V)$. Then

$$\langle\nu_i\rangle=2\pi\nu_c RJ_i(2e/m)^{\frac{1}{2}}(u_e\beta)^{5/2}/S^{V+1}, \tag{52}$$

where

$$\begin{aligned}J_i=h_i\{&[1-Sd/V-y_i/V\\&+Sdy_i/V(V-1)][1-I(y_i;V)]\Gamma(V+1)\\&-(y_i{}^V/\exp y_i)[Sdy_i/V(V-1)\\&-(y_i/V)+Sd/V(V-1)]\}.\end{aligned} \tag{53}$$

The values of $D_-$, $\mu_-$, and $\langle\nu_i\rangle$ are now substituted in Eq. (21), which is a transcendental equation involving $p/E_e$, $E_e\Lambda$, and $u_s$. By this method $D_-/\mu_-$ is also determined; it can thus be demonstrated that $D_-/\mu_-$ is practically independent of $u_s$, and is a function of $p/E_e$ alone, as is shown in reference 2.

Once this fact is established, a second and somewhat less laborious method may be used. It consists in evaluating Eq. (12), after insertion of $f$. The integral has a value at the lower limit, and one obtains

$$\langle\nu_{xi}\rangle+\langle\nu_i\rangle=\pi(2e/m)^{5/2}(u_e\beta)^{\frac{1}{2}}E_c{}^2/3\nu_c, \tag{54}$$

where $\langle\nu_{xi}\rangle=\langle\nu_x\rangle+\langle\nu_i\rangle$. In principle the two methods are related through integration by parts; but the approximation made in Eq. (37) will, in practice, introduce small and different errors. $\langle\nu_i\rangle$ is given in Eq. (52); $\langle\nu_x\rangle$ and $J_x$ are identical with Eqs. (52) and (53), with the subscript $x$ rather than $i$. Equation (54) becomes

$$2u_e\beta^2R(J_x+J_i)/\sigma S^{V+1}=1. \tag{55}$$

This is again a transcendental equation in $p/E_e$, $E_e\Lambda$, and $u_s$. Through Eq. (21), and A-R, one obtains the desired relation between $p/E_e$, $E_e\Lambda$ and $N_0\Lambda^2$.

## V. EXPERIMENTAL PROCEDURE

A block diagram of the experimental apparatus is shown in Fig. 1. The discharge cavity is constructed of OFHC copper. It is a right circular cylinder with a radius of 3.57 cm and a height of 0.635 cm that gives a resonant wavelength of 9.4 cm in the $TM_{010}$ mode, and

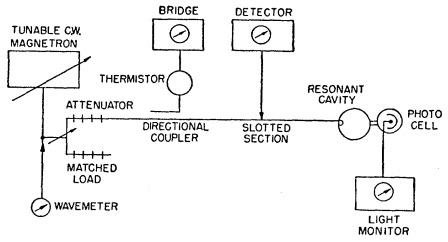


FIG. 1. Block diagram of the microwave system.

a diffusion length of 0.200 cm. Hydrogen can be admitted either through a heated palladium leak tube or directly from flasks of spectroscopically pure gas. A liquid nitrogen trap isolates the cavity and leak tube from all parts of the vacuum system which cannot be outgassed at temperatures above 300°C. The vacuum system can be pumped to pressures of the order of $10^{-8}$ mm Hg.

Experiments were performed in hydrogen in the pressure range 0.5–20 mm Hg. The procedure for each run was as follows: The gas was admitted to the desired pressure, and the discharge was initiated by adjusting the incident power level with the power divider. The light output of the discharge, monitored by a photocell, was noted. The magnetron frequency was then varied, the incident power being adjusted so that the light output was the same. At each frequency, the standing wave ratio and position of the voltage minimum on the slotted section, and the incident power, as read on the thermistor bridge, were recorded. In this way, a part of the resonance curve of the cavity plus discharge was determined. The electron density (and light output) was then set to a new value by changing input power, and the measurements were repeated. These measurements, plus the known characteristics of the empty cavity, suffice to determine the maintaining electric field and electron density.[8]

The measurements give both the discharge conductance $g_d$ and susceptance $b_d$. The ratio is

$$\frac{g_d}{b_d}=\int_0^\infty\frac{u^{\frac{1}{2}}\nu_c}{(\nu_c{}^2+\omega^2)}\frac{df}{du}du\Big/\int_0^\infty\frac{u^{\frac{1}{2}}\omega}{(\nu_c{}^2+\omega^2)}\frac{df}{du}du, \tag{56}$$

as can be seen from the integral over the velocities of Eq. (6). This gives the ac current which, in turn, is directly related to the complex conductivity of the plasma through Eq. (8) of Part III of reference 8. The right side of Eq. (56) is a weighted average $\langle\nu_c\rangle/\omega$. The present measurements yield, for hydrogen,

$$\langle\nu_c\rangle=4.85\times10^9p\ \text{sec}^{-1}\pm2\ \text{percent}.$$

The value is constant over the range $0.01<p/E_e<0.10$ cm×mm Hg/volt covered in this experiment. The probability of collision $P_c=\nu_c/pv$ for hydrogen, above 4 ev is proportional to $1/v$, and in that region $\nu_c\approx5.9\times10^9p$; below this value it is approximately constant. If the actual value of $\nu_c(v)$ is averaged over the distribution functions of Sec. IV, a value close to $4.85\times10^9p$ results for all values of $E_e/p$ experimentally realized.

The experimental results, obtained in a $TM_{010}$ mode cavity, do not correspond exactly to results that would be obtained in a plane-parallel system of infinite extent. Two corrections must be made. The first takes into account the radial variation of the applied field. The field varies with radius $r$ as $J_0(2.405r/R)$, where $J_0$ is

[7] K. Pearson, *Table of the Incomplete Gamma Function* (Cambridge University Press, Cambridge, 1946).

[8] S. C. Brown and D. J. Rose, J. Appl. Phys. **23**, 711, 719, 1028 (1952).

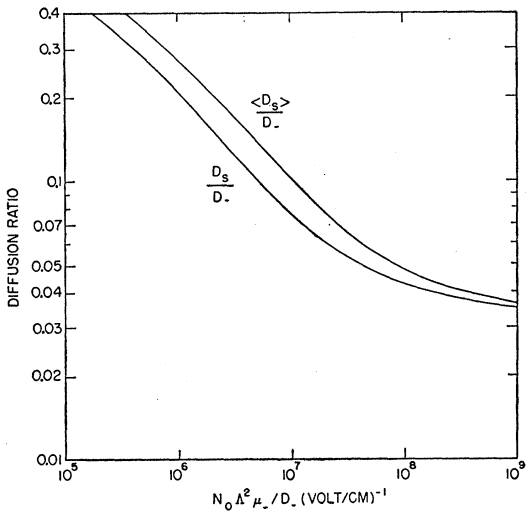


FIG. 2. Theoretical calculation of the quantities $D_s/D_-$ and $\langle D_s\rangle/D_-$ as a function of $N_0\Lambda^2\mu_-/D_-$.

the zero-order Bessel function, and $R$ is the cavity radius. The measured field at the center must be decreased slightly to correspond to the equivalent constant field throughout the cavity. The data are therefore corrected according to the theory of Herlin and Brown,[9] the correction amounting to no more than 5 percent.

The second correction arises because the plasma density itself has a radial variation, and this introduces a variable $D_s$ for diffusion to the ends of the cylinder. If the field were uniform, a radial dependence of $N$ and $P$,

$$\begin{Bmatrix} N \\ P \end{Bmatrix} = \begin{Bmatrix} N_0 \\ P_0 \end{Bmatrix} J_0(2.405r/R), \tag{57}$$

would be correct at both the free and ambipolar limits, and approximately correct in the transition region. Since the height of the cavity is much less than its radius, it is possible to define an average $\langle D_s\rangle$ for the discharge. It is

$$\langle D_s\rangle = \frac{\text{(Total electron flow to the walls)}}{\text{(Total number of electrons present)}} \times \Lambda^2$$

$$= \int_0^R D_s(N)N(r)2\pi r dr \Big/ \int_0^R N(r)2\pi r dr. \tag{58}$$

Allis and Rose give the quantity $D_s/D_-$. The integration can be performed graphically, to give $\langle D_s\rangle/D_-$ *vs* $N_0$, the electron density at the center of the cavity both radially and longitudinally. Figure 2 shows the quantities $D_s/D_-$ and $\langle D_s\rangle/D_-$ *vs* $N_0\Lambda^2\mu_-/D_-$ computed in this manner.

The theoretical results for hydrogen are shown in Fig. 3, where contours of constant $N_0\Lambda^2$ are plotted on the $p/E_e - E_e\Lambda$ plane. The contour $N_0\Lambda^2=0$ represents breakdown, and the contour $N_0\Lambda^2=\infty$ represents ambipolar diffusion. At large values of $N_0\Lambda^2$ ($\gtrsim 10^8$) and intermediate to small values of $p/E_e$ ($<0.05$) the calculations have not been made sufficiently exactly to warrant their inclusion in this figure. The difficulty may be traced to the approximation Eq. (37) made in solving the tail of the distribution function. The following parameters pertaining to hydrogen have been used in the calculation:

(a) $\nu_c = 4.85\times 10^9 p$ sec$^{-1}$ ($p$=mm Hg);

(b) $u_x = 8.9$ ev. This choice is explained by Ramien[10] on a quantum-mechanical basis.

(c) $u_i = 16.2$ ev.

(d) $h_x = h_i = 1.1\times 10^{-2}$ (volts$^{-1}$). These quantities are adjusted so that the products $\nu_c h_x(u-u_x)$ and $\nu_c h_i(u-u_i)$ are in agreement with the published values of the probabilities of excitation and ionization.

(e) $\mu_+/\mu_- = 32$. The value $\mu_+ = 14.7$ cm$^2$/volt-sec at 760 mm Hg and 18°C given by Tyndall[11] is used. This value is constant over the dc range $0 < E/p < 20$ volts/cm-mm Hg, and should be independent of the microwave field. Allis and Rose show that the dc space charge $E/p$ is less than the upper limit except in the immediate vicinity of the walls for a few combinations of high electron density and low pressure. Since $\mu_- = e/m\nu_c$ for constant $\nu_c$ we have at 18°C, in mks units, $\mu_+ = 1.12/p$, $\mu_- = 36/p$.

(f) $D_+\mu_-/D_-\mu_+ = 0$, an approximation justified by A-R.

Figure 4 shows the theoretical results of Fig. 3 plotted as a surface in $E_e\Lambda$, $p/E_e$, $N_0\Lambda^2$ space. The surface in the region of large $N_0\Lambda^2$ and small $E_e\Lambda$ has

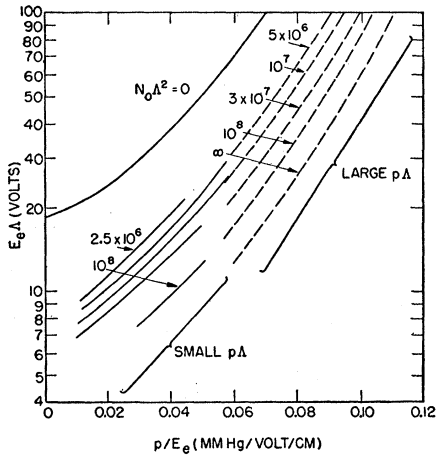


FIG. 3. Theoretical results for hydrogen where contours of constant $N_0\Lambda^2$ (in units of cm$^{-1}$) are plotted on the $p/E_e - E_e\Lambda$ plane.

[9] M. A. Herlin and S. C. Brown, Phys. Rev. **74**, 1650 (1948).

[10] H. Ramien, Z. Physik **70**, 353 (1931).

[11] A. M. Tyndall, *The Mobility of Positive Ions in Gases* (Cambridge University Press, Cambridge, 1938).

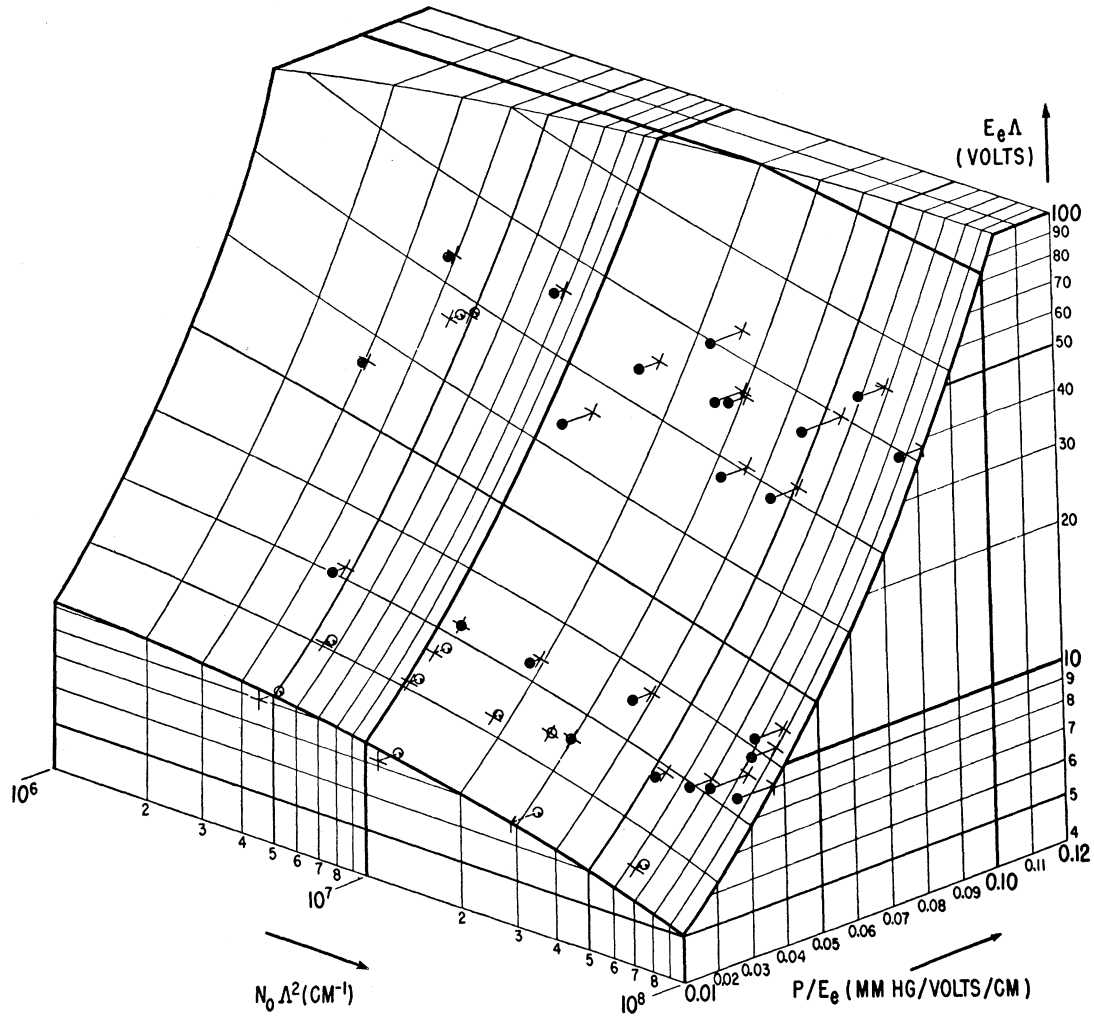


FIG. 4. A theoretical surface on which the experimental results are plotted. The experimental points are shown as dots, and their projections in the $p/E_e$ direction into the theoretical plane as crosses.

been obtained by extrapolation of the theoretical calculations of Fig. 3. The experimental points are shown as dots; their projection in the $p/E_e$ direction onto the theoretical plane, as crosses. The average of the experimental points is in good agreement with the theory (within 10 percent) both at large $E_e\Lambda$ and near $E_e\Lambda = 10$. At the lowest values of $E_e\Lambda$ and $p/E_e$, the electronic mean free path is about equal to the diffusion length, and diffusion theory can no longer be applied. The discrepancy at intermediate values, amounting at worst to about 20 percent in $p/E_e$ near the ambipolar limit, may be traced to the approximation made in solving the tail of the distribution function. In this region, near the ambipolar limit, the high pressure approximation begins to fail, and the asymptotic expansion Eq. (37) converges slowly. In each case, the error tends to raise $p/E_e$ for a given $E_e\Lambda$. The experimental error is believed to be about six percent.